Chapter 3. Millimeter-wave, Terahertz, and Infrared Devices

Academic and Research Staff

Professor Qing Hu

Visiting Scientists and Research Affiliates

Dr. Gerhard de Lange

Graduate Students

Erik K. Duerr, Kostantinos Konistis, Ilya Lyubomirsky, Arifur Rahman, Brian P. Riely, Benjamin S. Williams, Bin Xu, Noah D. Zamdmer

3.1 Introduction

Millimeter-wave and THz frequencies (f > 100 GHz) remain one of the most underdeveloped frequency ranges, even though the potential applications in remote sensing, spectroscopy, plasma diagnostics, and communications are obviously great. This is because the millimeter wave and far-infrared frequency range falls between two other frequency ranges in which conventional semiconductor devices are usually operated. One is the microwave frequency range, and the other is the near-infrared and optical frequency range. Semiconductor devices which utilize the classical diffusive transport of electrons, such as diodes and transistors, have a high frequency limit. This limit is set by the transient time and parasitic RC time constants. Currently, electron mobility and the smallest feature size which can be fabricated by lithography limit the frequency range to below several hundred GHz. Semiconductor devices based on quantum mechanical interband transitions, however, are limited to frequencies higher than those corresponding to the semiconductor energy gap, which is higher than 10 THz for most bulk semiconductors. Therefore, a large gap exists from 100 GHz to 10 THz in which very few devices are available.

Semiconductor quantum-effect devices (which can be loosely termed "artificial atoms"), including both vertically grown quantum-well structures and laterally confined mesoscopic devices, are human-made quantum mechanical systems in which the energy levels can be chosen by changing the sizes of the devices. Typically, the frequency corresponding to the intersubband transitions is in the millimeter-wave range (ΔE ~ 1-4 meV) for the lateral quantum-effective devices, and THz to infrared for the vertical quantum wells. It is therefore appealing to develop ultrahigh-frequency devices, such as radiation detectors and mixers, and THz and infrared lasers utilizing the intersubband transitions in these devices.

In addition to new physical concepts, novel technologies must also be developed to meet the challenges at these high frequencies. Conventional mechanically machined horn antennas integrated with waveguide cavities have been the workhorse at microwave and millimeter-wave frequencies since they were first implemented more than fifty years ago during World War II. Very high antenna gain and essentially perfect antenna efficiency can be achieved using these structures. However, they are expensive, bulky, and incompatible with arrays. In order to overcome these problems, new development has been made to use micromachining to fabricate the horn antenna structures.

In these structures, the active elements and their planar antennas are fabricated on a free-standing thin (~1 micron) SiN membrane, which is suspended over a silicon pyramidal horn that is formed by anisotropic etching, which is known as micromachining. The side walls of this micromachined structure can then be coated with gold to form a horn antenna. Compared to conventional waveguide horn antennas, this novel micromachined structure has several major advantages. It is easier to fabricate fine three-dimensional structures by using photolithography. Horn antennas with micron precision can be easily defined and inexpensively mass produced. This kind of antenna is made on Si or GaAs wafers and compatible with thin-film technology. Thus, active elements, such as RF and IF amplifiers, mixers and video detectors, local oscillators, and post-detection signal processors, can be integrated monolithically with the antenna structures to form monolithic transmitter/receiver systems. The micromachined antenna is light-weight and compact.

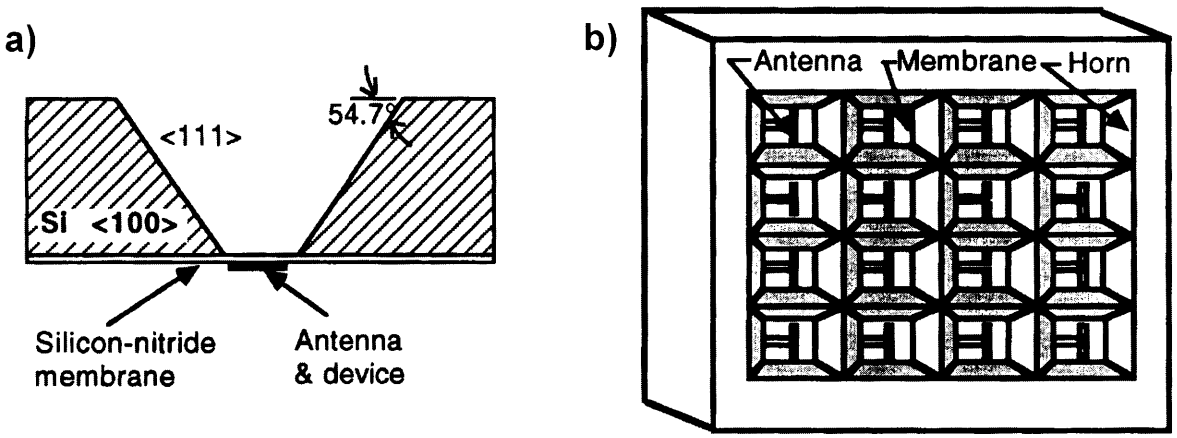

Figure 1. (a) Example of a micromachined horn antenna structure that is made by anisotropically etching a <100> silicon wafer. (b) Schematic of a focal-plane array on a single wafer made using micromachining.

The most attractive feature of the micromachined structure is that focal-plane arrays can be fabricated easily on a single wafer, as illustrated in Figure 1b. Such systems will yield a significantly improved spatial resolution in remote sensing and a much greater antenna gain when implemented with phased-arrays.

In our group, we are systematically investigating physical and engineering issues that are relevant to devices operating from millimeter-wave to infrared frequencies. Specifically, we are working on micromachined millimeter-wave focal-plane arrays and development of terahertz and infrared lasers based on intersubband transitions.

3.2 Micromachined SIS Millimeter-wave Focal-plane Arrays

Sponsors

National Aeronautics and Space Administration
Grant NAGW-4691
National Science Foundation
Grant AST 94-23608

Dr. Gerhard de Lange, Arifur Rahman, Erik K. Duerr, Kostantinos Konistis, Professor Qing Hu, in collaboration with Dr. Gerry Sollner and Group 86,[1] Dr. Arthur Lichtenberger,[2] Dr. Ray Robertazzi,[3] and Dr. David Osterman[4]

Superconductor-insulator-superconductor (SIS) heterodyne receivers have been demonstrated to be the most sensitive receivers throughout 30-840 GHz frequency range. The challenge now in the SIS receiver technology is to develop focal-plane arrays to improve the efficiency of data acquisition. In order to achieve these goals, we are currently developing a novel scheme to couple the millimeter-wave and infrared signals to the superconducting devices by using a micromachined horn antenna and a planar antenna supported by a thin (~1 micron) membrane, as shown in Figure 1a. As stated in the introduction, this novel micromachined antenna structure can be

1 MIT Lincoln Laboratory, Lexington, Massachusetts.

2 University of Virginia, Charlottesville, Virginia.

3 Hypres, Inc.

4 Ibid.

produced with a high precision using photolithography, and it can be utilized in focal-plane arrays, as shown in Figure 2b.

Following our recent success in developing single-element micromachined SIS receivers [see our previous publication in *Applied Physics Letters* 68: 1862 (1996)], we have designed and constructed a 3x3 focal-plane array with the center frequency around 200 GHz. The schematic of the structure is shown in Figure 2a, which includes a micromachined and mechanically machined horn array, the device wafer, and the dc and IF connection board. Preliminary measurements of the dc I-V characteristics showed good uniformity across the entire array. Figure 2b shows the I-V curves from seven SIS junctions in the array. The resistance variation of these junctions is within 5%. Our heterodyne mixing measurement on a center element yielded a receiver noise as low as 50 K (DSB) at 190 GHz with a 3 dB bandwidth of 25 GHz. This result is comparable to the best achieved from conventional waveguide SIS receivers. We are currently in the process of measuring both the video and heterodyne response of the entire focal-plane array. Our next step will be to integrate on-chip Josephson-junction local oscillators with the SIS mixers to form monolithic focal-plane arrays.

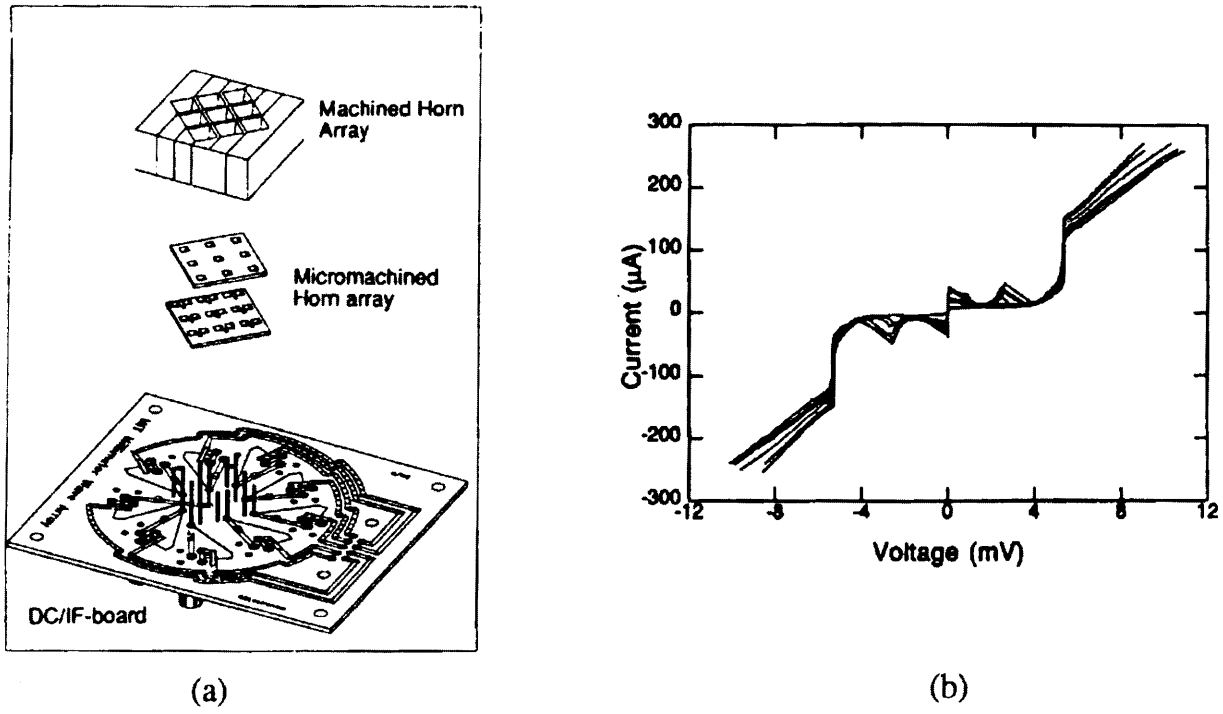

Figure 2. (a) Schematic of an array structure including a micromachined and machined horn array, the device wafer, and the dc and IF connection board. (b) I-V curves of seven SIS junctions in the array.

3.3 Intersubband-transitions Lasers

3.3.1 Electrically Pumped THz Emitters using Quantum Wells

Sponsor

U.S. Army Research Office
Grant DAAH04-95-1-0610

Project Staff

Bin Xu, Professor Qing Hu, in collaboration with Dr. Michael R. Melloch[5]

Semiconductor quantum wells are human-made quantum mechanical systems in which the energy levels can be designed and engineered to be of any value. Consequently, unipolar lasers based on intersubband transitions (electrons that make lasing transitions between subband levels within the conduction band) were proposed for long-wavelength sources as early as the 1970s. However, because of the great challenge in epitaxial material growth and the unfavorable fast nonradiative relaxation rate, unipolar intersubband-transition lasers (also called quantum-cascade lasers) at near-infrared (4-5 micron) and mid-infrared (8-11 micron) wavelengths were developed only recently at Bell Laboratories.

This achievement is remarkable, but the technique used in the original quantum-cascade lasers will not be directly applicable for the longer-wavelength THz range because of two major obstacles. First, the energy levels corresponding to THz frequencies (1 THz = 4 meV) are quite narrow, so the requirements for the design and fabrication of suitable quantum wells are demanding. Because of the narrow separation between subband levels, heating and hot-electron tunneling will have a much greater effect. Also, the small energy scales of THz photons make the detection and analysis of spontaneous emission (a crucial step toward developing lasers) quite difficult. Second and perhaps the most important, mode confinement, which is essential for any laser oscillation, is difficult at longer wavelengths. Conventional dielectric-waveguide confinement is not applicable because the evanescent field penetration, which is proportional to the wavelength and is on the order of several tens of microns, is much greater than the active gain medium of several microns.

We are currently developing intersubband-transition lasers based on our recent success in generating and detecting THz emission signals and on a novel mode confinement method using metallic waveguide structures.

Our MQW structure for THz emission is shown in Figure 3, in which the conduction band profile and the square of the wave functions were calculated self-consistently from Schrödinger and Poisson equations. The device is formed by a triple-well structure using $GaAs/Al_{0.3}Ga_{0.7}As$ materials, as shown in the dashed box. This structure is essentially a three-level system (marked as E_3, E_2, and E_1 in Figure 3; the level E_4 is much higher in energy so it does not contribute to transport at low biases), which is required for any lasers. Because there is no recombination involved in unipolar intersubband lasers, electrons can be "reused" many times. Consequently, many identical triple-well modules can be cascade-connected, and the emission power and the mode confinement factor can be increased substantially.

Due to translational symmetry, design analysis needs to focus only on one module, provided there are no global space charges and high-field domains. The collector barrier (the one with a 2.0-nm thickness) is center δ-doped at approximately $10^{11}/cm^2$ in order to provide dynamic charges to assure a global charge neutrality. The radiative transition takes place between E_3 and E_2, with an energy separation of $\Delta E_{32} \approx 14$ meV and an oscillator strength of $f_{32} \approx 0.31$ (using the effective mass in GaAs). Under the designed bias of 50 mV per module, the ground state E'_1 of a previous module is aligned with E_3. Thus, the upper subband E_3 can be selectively populated through resonant tunneling. The energy separation between E_2 and E_1 was designed to be 36 meV under the bias, which corresponds to the LO-phonon energy $\hbar\omega_{LO}$ in GaAs. Once energetically allowed, the very fast LO-phonon scattering (with a time $\tau 21 \approx 1.4$ ps) will rapidly depopulate the E_2 level and establish a population inversion between E_3 and E_2.

5 Purdue University, West Lafayette, Indiana.

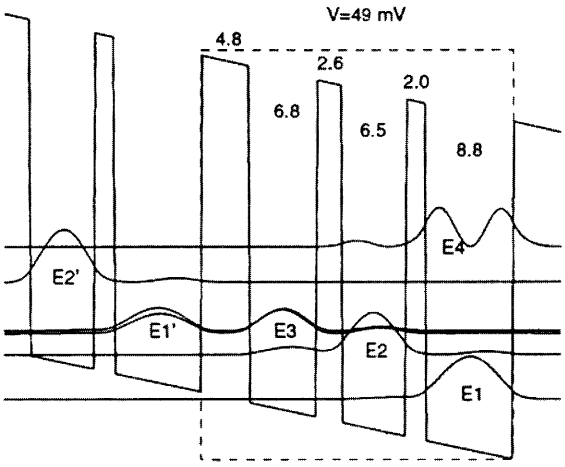

Figure 3. Schematic of a three-level system based on a triple quantum-well structure. The radiation transition takes place between E_3 and E_2, and the fast LO-phonon emission keeps the level E_2 empty. The conduction-band profile and the square of the electron wavefunctions were calculated numerically from Schrödinger and Poisson equations.

The MQW structures were grown in the molecular-beam epitaxy (MBE) machine in the group of our collaborator Professor Michael R. Melloch at Purdue University. In order to verify the accuracy of our design calculations and to inspect the quality of quantum wells and interfaces, we performed an infrared absorption measurement with the result shown in Figure 4. The measurement was performed on a 80-module device (with a total of 240 quantum wells) at room temperature. A mid-infrared absorption peak is clearly seen at 110 meV, which is due to the intersubband transition from E_1 to E_4. The FWHM is only 7 meV, including a 4-meV instrumental linewidth. This narrow linewidth is an indication of the high quality and uniformity of the wells and interfaces. Furthermore, the measured E1→E4 transition frequency of 110 meV and the dipole moment of 14 Å (deduced from the area of the absorption peak) agreed quite well with the calculated values of 109 meV and 12 Å, indicating the accuracy of our calculations.

In order to measure the intersubband THz emission and resolve its spectra, we constructed a set-up that included an external Fourier transform infrared spectrometer (FTIR) with a composite Si bolometer as its detector. The system's schematic is shown in Figure 5. We have improved this system and perfected our measurement techniques so that THz emission measurements can be routinely performed on our emitters with output power levels of 1-10 nW.

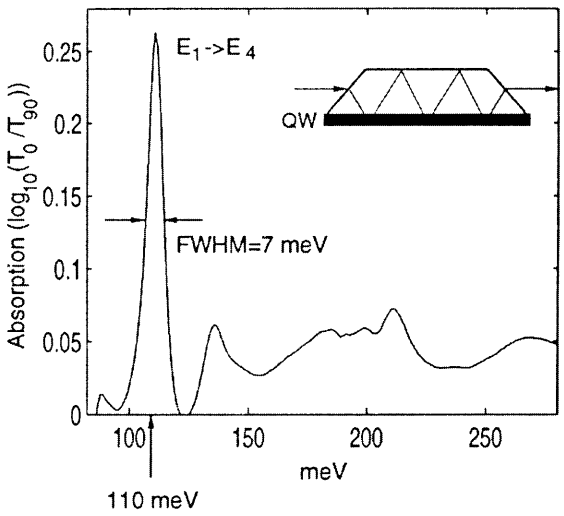

Figure 4. Infrared absorption measurement of a 80-module device, which was placed at room temperature. The absorption peak is due to the E1→E4 intersubband transition. The measured FWHM is 7 meV, including a 4-meV instrumental linewidth. The measured intersubband transition frequency (110 meV) and dipole moment (14 Å) agreed quite well with the calculated values of 109 meV and 12 Å.

Using the emission measurement system shown in Figure 5, we resolved the emission spectra from many different MQW devices and at different biases. A representative one is shown in Figure 6. This result was obtained from a 10-module device using a metallic grating with a period of 10 micron for surface emission. At a bias of 0.55 V, which is slightly higher than the designed value (0.5 V for 10 modules), the emission spectrum exhibits two peaks at 26 meV and 40 meV. The FWHM for both peaks is approximately 5 meV (including a 4-meV instrumental linewidth). According to our simulation, the lower emission peak is due to the $E_3 \rightarrow E_2$ transition, and the higher one is due to the $E_2 \rightarrow E_1$ transition. One important conclusion that can be drawn from this spectrum is the relative subband populations. Similar to the absorption measurement discussed earlier, the area of an emission peak is proportional to the product of the oscillator strength and the upper-level electron population. Our calculation indicated that the two transitions $E_3 \rightarrow E_2$ and $E_2 \rightarrow E_1$ have comparable oscillator strengths ($f_{32} = 0.31$ and $f_{21} = 0.27$). In Figure 6, the area of the $E_3 \rightarrow E_2$ peak is approximately twice that of the $E_2 \rightarrow E_1$ peak, thus yielding an inverted population condition $n_3 \approx 2n_2$. We believe this to be the first observation of inverted populations in electrically

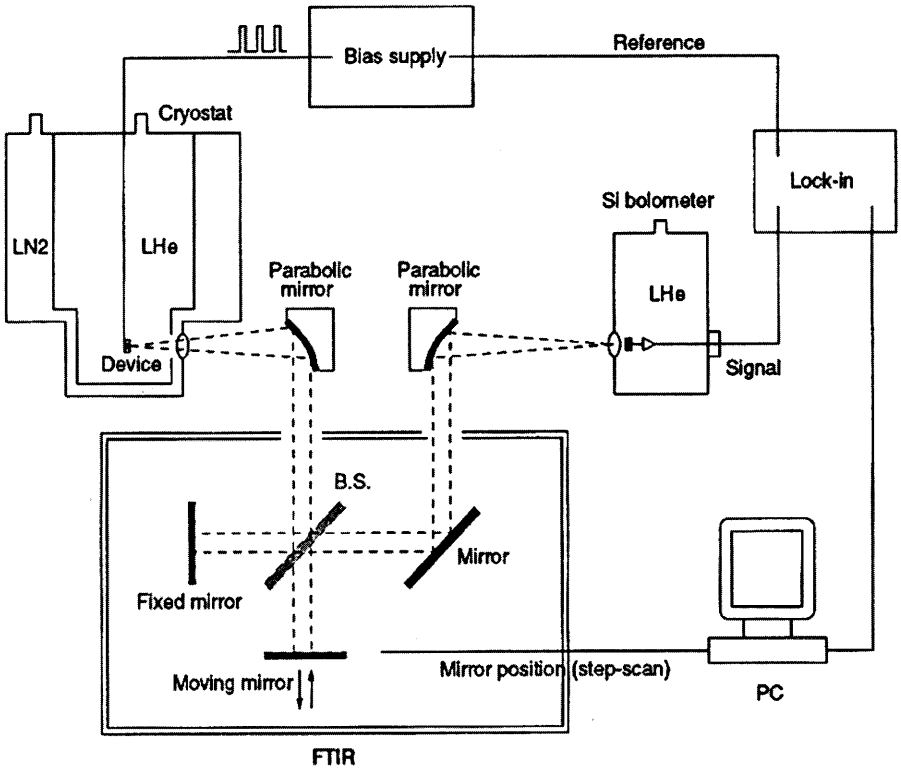

Figure 5. Far-infrared measurement set-up that uses an external Fourier transform spectrometer to spectrally resolve the emitted THz signals.

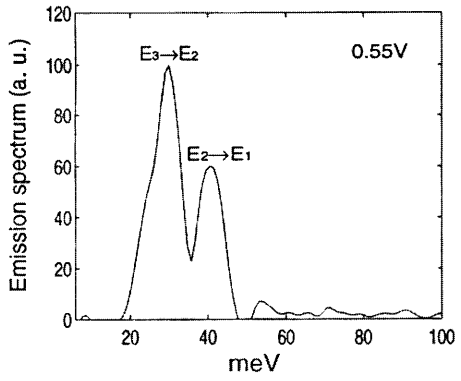

Figure 6. THz emission spectrum from a 10-module device. The device is submerged in liquid helium and the total bias is 0.55 V. The lower emission peak at 26 meV is attributed to the $E_3 \rightarrow E_2$ transition, and the higher peak at 40 meV is due to the $E_2 \rightarrow E_1$ transition. The FWHM of both peaks is approximately 5 meV including a 4-meV instrumental linewidth.

pumped intersubband THz emitters, and is a promising indication of the feasibility of THz lasers based on intersubband transitions.

3.3.2 Optically Pumped THz Emitters using Quantum Wells

Sponsors

AASERT/U.S. Army Research Office
Grant DAAH04-94-G-0167
Hertz Foundation Fellowship

Project Staff

Ilya Lyubomirsky, Professor Qing Hu, in collaboration with Dr. Michael R. Melloch[6]

Compared to electrical pumping, optical pumping offers advantages of an easier design, a higher selectivity in pumping, and a separation of the pump and electrical bias. For THz emitters, easily available CO_2 lasers can be used as the pumping source. We

6 Professor, Purdue University, West LaFayette, Indiana.

first designed a three-level system for THz emission. However, this structure showed an excessive heating when it is pumped by an intense CO_2 laser. In order to increase the emission efficiency and therefore the gain of the active medium, we have redesigned our optically pumped THz emitters based on a four-level system using coupled triple quantum wells, as shown in Figure 7. Electrons on the ground state E_1 can be pumped by a CO_2 laser to the E_4 level. By carefully engineering the scattering rates between subband levels by choosing subband energy separations and spatial locations, a population inversion between E_3 and E_2 can be achieved. It was estimated that a modal gain of approximately 100 cm^{-1} can be achieved at a 1-W average pump power level.

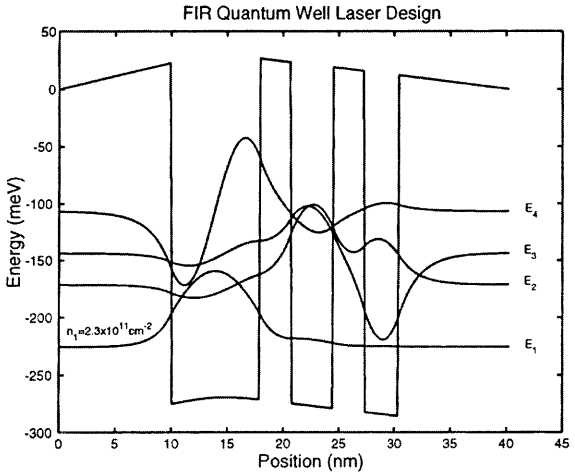

Figure 7. Schematic of a four-level system based on a coupled triple quantum-well structure. Electrons can be pumped from the E_1 to the E_4 level by a CO_2 laser. They then quickly relax to the E_3 level by LO-phonon scattering. Similarly, the electrons on the E2 level can be emptied quickly to E_1 through LO-phonon scattering. THz emission is to take place between E_3 and E_2.

3.3.3 Mid-infrared Quantum-cascade Lasers

Sponsor

U.S. Army Research Laboratory - Federated Laboratories
Grant QK-8819

Project Staff

Benjamin S. Williams, Brian P. Riely, Professor Qing Hu, in collaboration with Dr. Michael R. Melloch

High-power, compact mid-infrared (8-12 micron) lasers are very useful tools for remote sensing, end-point detection in dry etching processes, point-to-point communication, and night vision applications. Conventional laser diodes operating in this long wavelength range use narrow-gap lead-salt semiconductors, which require cryogenic operations, provide relatively low power levels, and have very limited frequency tunability. Recently developed quantum-cascade (QC) lasers based on intersubband transitions have shown much higher operating temperatures and a great frequency tunability. These features make them ideal for the above-mentioned applications. In this project, we are developing mid-infrared quantum-cascade lasers based on GaAs/AlGaAs quantum-well structures. Compared to the InGaAs/InAlAs materials used in the original quantum-cascade lasers developed at Bell Labs, the GaAs/AlGaAs system offers a much higher thermal conductivity (approximately a factor of 20 compared to InGaAs/InAlAs) and therefore a higher-power operation.

The core of our MQW structure is a tightly coupled double quantum well, in which three energy levels form the three-level lasing structure. These energy levels are shown in Figure 8. The lasing transition is to take place between E_3 and E_2, with the energy separation approximately 120 meV, corresponding to 10-micron wavelength. The energy separation between E_2 and E_1 is designed to be approximately 36 meV, which is the energy of LO phonon in GaAs. Consequently, the energy level E_2 will be depopulated by very fast LO-phonon scattering (~ 0.2 ps). Our design of the MQW structures is aided by a numerical code that solves Shrödinger and Poisson equations self-consistently, and it includes the effect of band nonparabolicity to account for the much higher energy levels corresponding to infrared frequencies.

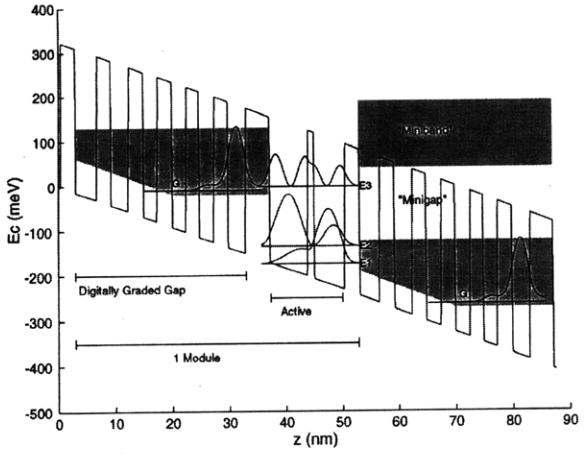

Figure 8. Conduction-band profile and wave functions of the designed MQW structure that contains a three-level gain medium and superlattices for selective injection and removal of electrons.

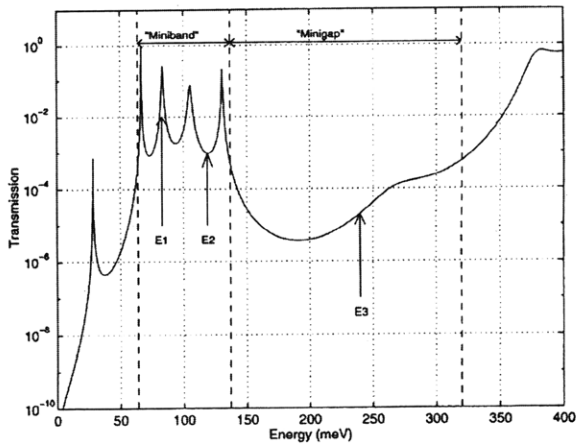

Figure 9. Calculated transmission coefficient of the superlattice sandwiching the core structure. The valley in the transmission corresponds to the minigap, and the peaks form the miniband.

The superlattice structure sandwiching the active region serves the purpose of selective injection of electrons into the E_3 level, and selective removal of electrons from both E_2 and E_1 levels. By choosing the period of the superlattice properly, the Bragg reflection results in minigaps (transport forbidden) and minibands (transport allowed), as shown in both Figure 8 and Figure 9. The combination of the selective injection into E_3 and the fast removal from E_2 will assure an inverted population between these two levels. We calculated the dipole moment for the $E_3 \rightarrow E_2$ transition to be approximately 23 Å, which yields a modal gain of 480 cm^{-1} for a doping concentration of 1.5 $10^{11}/cm^2$. Such a high level of gain is characteristic of the QC lasers in which the two subbands track each other in momentum, resulting in a large joint density of states.

We have fabricated an MQW structure consisting of 40 nominally identical structures as shown in Figure 8. We have performed emission measurements using the FTIR system shown in Figure 5. An emission spectrum with the narrowest linewidth is shown in Figure 10. The center frequency of 121 meV (corresponding to 10-micron wavelength) is what we designed for, and the FWHM linewidth is only 10.8 meV. This linewidth is comparable to the narrowest achieved at Bell Labs using InGaAs/InAlAs structures, and is an indication of the high interface quality and uniformity of our MQW structures. Currently, we are designing suitable cladding layers for mode confinement to achieve lasing.

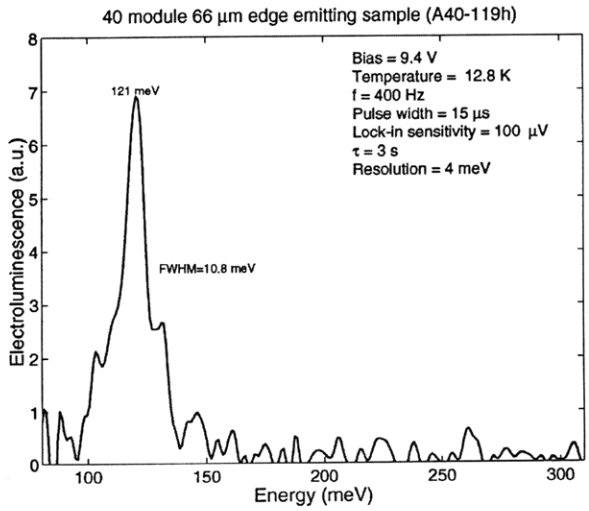

Figure 10. Spectrum of spontaneous intersubband emission from a 40-module MQW structure whose design is shown in Figure 8.

3.4 Publications

3.4.1 Journal Articles

del Alamo, J.A., C.C. Eugster, Q. Hu, M.R. Melloch, and M.J. Rooks. "Electron Waveguide Devices." *Superlatt. Microstruct.* 23: 121 (1998).

Lyubomirsky, I., and Q. Hu, "Optical Parametric Oscillators Without Phasematching." *J. Opt. Soc. Amer. B* 14: 984 (1997).

Lyubomirsky, I., B. Xu, and Q. Hu. "Developing Quantum-well Sources of Terahertz Radiation." *IEEE-LEOS News.* 11: 13 (1997).

Verghese, S., N. Zamdmer, Q. Hu, and A. Foerster. "Cryogenic Picosecond Sampling using Fiber-coupled Photoconductive Switches." *Appl. Phys. Lett.* 70: 2644 (1997).

Xu, B., Q. Hu, and M.R. Melloch. "Electrically Pumped Tunable Terahertz Emitter Based on Intersubband Transition." *Appl. Phys. Lett.* 70 (1997).

Xu, B., and Q. Hu, "Grating Coupling for Intersubband Emission." *Appl. Phys. Lett.* 70: 2511 (1997).

3.4.2 Chapter in a Book

Xu, B., Q. Hu, and M. R. Melloch. "Intersubband THz Emission in Multiple Quantum Wells." Chapter 10, "Long Wavelength Infrared Emitters Based on Quantum Wells," vol. 9 in *Optoelectronic Properties of Semiconductors and Superlattices.* Ed. M. Helm. New York: Gordon and Breach. Forthcoming.

3.4.3 Conference Papers

de Lange, G., Q. Hu, H. Huang, and A. W. Lichtenberger. "Development of a 170-210 GHz 3x3 Micromachined SIS Imaging Array." Paper presented at the 8th International Symposium on Space Terahertz Technology, Cambridge, Massachusetts, March 1997; published in the symposium proceedings, pp. 518, 1998. Also presented at the 20th ESTEC Antenna Workshop on Millimeter Wave Antenna Technology and Antenna Measurements, Noordwijk, the Netherlands, June 18-20. 1997; to be published in the workshop proceedings.

Hu, Q., B. Xu, and M.R. Melloch. "Intersubband Terahertz Emitters." Paper presented at the International Workshop on Intersubband Transitions in Quantum Wells: Physics and Devices, Tainan, Taiwan, December 1997. (Invited paper delivered by H.C. Liu.)

Hu, Q. "High-frequency Dynamics of Antenna-coupled Mesoscopic Devices." Paper presented at the 1997 APS March meeting, Kansas City, Missouri, March 1997. Invited paper, session N2.01.

Lyubomirsky, I., Q. Hu, C. Hansing, and B.G. Streetman. "Terahertz Intersubband Emission in Optically Pumped Quantum Wells." Paper presented at the Material Research Society Fall Meeting, Boston, Massachusetts, December 1997.

Rahman, A., E. Duerr, G. de Lange, and Q. Hu. "Micromachined Room-temperature Microbolometer for mm-wave Detection and Focal-plane Imaging Arrays." Invited paper presented at SPIE Aerosense Symposium, Orlando, Florida, April 1997; published in *SPIE Proc.* 3064: 122 (1997).

Xu, B., B. Williams, Q. Hu, and M.R. Melloch. "Intersubband Terahertz Emission from Electrically Pumped Multiple Quantum Wells." Paper presented at 1997 Material Research Society Fall Meeting, Boston, Massachusetts, December 1997.

3.4.4 Thesis

Duerr, E.K. *Millimeter-wave Integrated Horn Antennas.* Department of Electrical Engineering and Computer Science, MIT, December 1997.